Fatigue Crack Propagation in Alloy 718: A Review

Lee A. James

Westinghouse Electric Corporation
P. O. Box 79
West Mifflin, PA 15122

ABSTRACT

The fatigue crack propogation (FCP) behavior of Alloy 718 is reviewed within the framework of linear elastic fracture mechanics. A wide variety of mechanical, material, and environmental variables are known to influence FCP behavior in Alloy 718, and the effects of these variables are reviewed herein.

INTRODUCTION

Alloy 718 is certainly one of the most widely used of the nickel-base superalloys. The alloy possesses excellent strength and creep resistance at elevated temperatures, and in some environments it possesses excellent corrosion resistance. For these reasons, it has enjoyed extensive use in the aerospace, nuclear, and petrochemical industries. In addition, because of its austenitic microstructure, Alloy 718 has excellent fracture and ductility properties at cryogenic temperatures, and hence has found applications in rocket motor casings and in superconducting structural applications.

Because of this widespread usage, much of which involves cyclic loadings, the fatigue crack propagation (FCP) behavior of Alloy 718 has been studied quite extensively. Scores of publications have dealt with the effects of various parameters upon the FCP behavior of Alloy 718, and it is the objective of the present paper to review these numerous publications. The sheer number of these publications necessitates that the review of each cannot be done in depth; hence the reader is encouraged to consult the individual publications for details that cannot be covered herein.

The various parameters influencing FCP in Alloy 718 can be characterized under three broad general categories: mechanical variables, material variables, and environmental variables, and this paper is organized in that fashion. The distinction between categories is, in some cases, blurred by the fact that many of the parameters are synergistic; e.g., temperature, cyclic frequency, environment and alloy microstructure can interact synergistically to produce a variety of FCP behaviors.

This paper concentrates on the crack extension behavior under cyclic loadings. Cracks readily propogate in Alloy 718 under static loadings at elevated temperatures, and although generally beyond the scope of this paper, results under static loadings will be reviewed when they can be related to similar cyclic loadings.

Superalloy 718—Metallurgy and Applications
Edited by E.A. Loria
The Minerals, Metals & Materials Society, 1989

MECHANICAL VARIABLES

Effect of Temperature

There is equal justification for classifying temperature as an environmental variable, but the effect of temperature is so closely related to many of the other parameters that it is discussed first. A number of studies have been devoted to the effects of temperature upon the FCP behavior of Alloy 718, and the majority of these have been in an air environment (1-17). As mentioned previously, Alloy 718 enjoys applications over a very wide range of temperatures, and this is evident by the wide range of experimental temperatures catalogued in Table I. With only one exception, all of the studies shown in Table I showed that, in an air environment*, FCP rates increased with increasing temperature. This trend has, of course, been observed most other alloy systems tested in an air environment. Typical behavior is illustrated in Figure 1 which is taken from the results of Reference 3. The one exception to the above trend are the results of Reference 5 where FCP rates at 760°C were slightly lower than those at 649°C. This was attributed to crack tip blunting at the very high temperature of 760°C. It should be pointed out that the highest precipitation temperature employed in most heat-treatments of Alloy 718 is 621°C. Hence, any tests conducted at temperatures in excess of 621°C will be in material which is undergoing overaging as the test proceeds, and the microstructure after testing at 760°C is likely to differ from that after testing at 649°C.

The main factor in increasing FCP rates in air as the temperature is thought to be oxygen, and this will be discussed in the later section or environmental variables. The entire increase is not due to the environment, however, as temperature effects are noted in elevated temperature vacuum environments, thereby suggesting a creep component. Reference 9 studied FCP behavior in vacuo at 24°, 538°, and 649°C. Crack growth rates increased slightly with increasing temperature, and could be correlated by plotting da/dN as a function of stress intensity factor range normalized by Young's Modulus ($\Delta K/E$). Reference 19 noted a similar slight increase in FCP rates in vacuo from 593°C to 649°C, and Reference 20 noted similar increases under static loads in vacuo at 538°, 649°, and 704°C.

Increases in FCP rates with increasing temperature in a pure hydrogen environment (133 kN/m^2 pressure) were noted in Reference 21 at temperatures of -52°, 24° and 303°C. (No crack extension was noted under static loads at 24°C with an applied K of 99 $MPa\sqrt{m}$). Clearly, the temperature effects noted in Reference 21 are not due to an oxygen interaction, and the temperatures are too low for a creep interaction.

Effect of Cyclic Frequency

A number of studies have dealt with the effect of cyclic frequency upon the FCP behavior of Alloy 718. In general, most of these studies have characterized frequency effects in an air environment (3, 14, 22-25), with very little study of other environments (23). Frequency effects are most pronounced at elevated temperatures and hence most studies have concentrated on characterizing this regime. References 3 and 22 studied frequency effects at 538°C over the range 1.39×10^{-3} Hz to 6.67 Hz, and the results shown in Figure 2 are typical for most observations: At

*At least part of the tests in References 1, 4, and 6 were conducted at cryogenic temperatures where the surrounding gaseous environment was either partially or wholly composed of gasses other than air (e.g., H_2, N_2, He, CO_2).

elevated temperatures, FCP rates increase with increasing temperature. Similar trends were noted in Reference 14 at 550°C over the range 5×10^{-3} Hz to 20 Hz, in Reference 23 at 650°C over the range 0.01 Hz to 1 Hz, and in Reference 24 at 650°C over the range 10^{-3} Hz to 50 Hz. Reference 25 studied the effect of frequency (0.01 Hz to 400 Hz) at 649°C upon the crack growth threshold, and this will be discussed in the later section on thresholds.

Reference 23 studied FCP behavior at 650°C over the range 0.01 Hz to 1 Hz in two environments: air and helium (99.995% purity). Relatively strong frequency effects were noted in the air environment while the effects in helium were relatively weak. Frequency effects in air are generally considered to be strongly influenced by environmental effects (specifically the oxygen in air [23]), but the weak frequency effects in helium suggest that a non-environmental component (probably creep) also plays a small role.

When crack growth rates at a constant value of ΔK are plotted versus cyclic frequency over a wide range of frequencies, three general regimes of frequency dependence are noted. This is illustrated in Figure 3 using data from Reference 24 for ΔK = 40 MPa/m at 650°C. At frequencies greater than 100 Hz, crack growth rates tend to be approaching a horizontal asymptote which would correspond to fully cycle-dependent behavior. At frequencies below about 0.01 Hz, the slope of the da/dN versus frequency curve approaches a slope of -1 which corresponds to fully time-dependent growth. Between these two extremes exists a regime of mixed time-dependent and cycle-dependent behavior. In general, each regime exhibits differing mechanisms of crack extension: striation formation is generally observed in the cycle-dependent regime, intergranular crack extension in the time-dependent regime, and mixed transgranular-intergranular crack extension in the mixed time- and cycle-dependent region.

In general, frequency effects are only observed at elevated temperatures and not at room temperature.

Wave Shape (or Hold-Time) Effects

Closely related to frequency effects is the subject of wave shape effects at elevated temperatures. Because structural loads are often held at or near the maximum value during fatigue cycling, a number of studies have been devoted to characterizing hold-time effects [5, 14, 22, 26-38]. In general, at elevated temperatures the addition of a hold-time at or near the maximum tensile portion of the loading cycle produces FCP rates that are faster than those for continuous cycling. Reference 22 studied two wave shapes in air at 538°C: a "positive sawtooth" (slow load rise, rapid load fall) and a "square wave" with a maximum tensile hold-time. Both waveforms had the same cyclic frequency (1.39×10^{-3} Hz), but the square wave (hold-time = 648 sec.) exhibited FCP rates approximately five times faster than the sawtooth wave. Hold-time effects have been studied extensively over the temperature range 538°C to 650°C, and in general, FCP rates increase with increasing hold-times (see, for example, Reference 26 where hold times at 538°C ranged between 90 seconds to 2 hours). Reference 35, studying hold-time effects at 649°C, found that hold-times greater than 5 seconds produced purely time-dependent behavior (i.e., the region of slope = -1 in Figure 3). On the other hand, Reference 29 found that, at 425°C, hold-times up to 10 minutes produced purely cycle-dependent behavior (i.e., the region of slope = 0 in Figure 3). Clearly, the effects of temperature and hold-time are synergistic.

Microstructural features (e.g., grain size) have only a moderate effect upon FCP behavior during continuous cycling, but References 22 and 31 have shown that grain size has a profound effect under hold-time conditions at elevated temperatures (see the later section on Microstructural Effects).

The effect of neutron irradiation upon FCP behavior will be covered in a later section, but it has been observed that hold times tend to accentuate irradiation effects at both 427°C [32] and 650°C [33, 37].

Only a few studies have dealt with hold-time effects in environments other than air. In this case, three studies [9, 19, 39] have reported on hold-time effects in vacuo, and the results are slightly contradictory. Reference 9 reported no difference in FCP rates in vacuo at 538°C between continuous cycling at 0.17 Hz and a 60-second hold time, but did note FCP rates at 650°C increasing from continuous cycling at 0.17 Hz to a 60-second hold-time to a 600-second hold-time. If the results at 650°C were plotted on a time basis (i.e., da/dt), all the data overlapped thereby suggesting purely time-dependent behavior. On the other hand, References 19 and 39 reported little or no difference in FCP rates in vacuo at 650°C between continuous cycling at 0.17 Hz and a 60-second hold-time.

Finally, a word of caution is in order about the validity of linear elastic fracture mechanics (LEFM) analysis methods under hold-time conditions at temperatures of approximately 650°C. Reference 30 employed a 15-minute hold-time at 650°C on three specimens as shown in Figure 4. Note that even though the maximum stress levels were well below the yield strength at this temperature (about 932 MPa), a unique correlation between da/dN and ΔK was not observed. The present author has made similar observations for Alloy 718 cycled at 538°C using a 10.8 minute hold-time. This clearly suggests a breakdown in the ability of LEFM methods to uniquely describe FCP rates under this condition. This will be discussed further in the section on crack growth under static loads.

Effect of Stress Ratio

Experimenters often find it convenient to conduct FCP tests at a stress ratio close to zero ($R = K_{min}/K_{max}$), yet in service, loadings generally occur at nonzero stress ratios. For this reason, a number of studies have dealt with stress ratio effects in Alloy 718 [1, 3, 15, 25, 27, 39, 40-43]. The range of stress ratios and temperatures that have been studied is summarized in Table II. The general trend noted in all of these studies is, that on a basis of ΔK, FCP rates at a given temperature increase with increasing R (the opposite trend is noted if crack growth rates are compared on a K_{max} basis). A large number of empirical relationships have been proposed to correlate stress ratio effects, but one of the simplest and widely employed is that proposed by Walker [44]. In this relationship K_{eff} replaces ΔK in the usual Paris power law such that

$$K_{eff} = K_{max} (1-R)^m \qquad \text{Eq. [1]}$$

where the exponent "m" is determined empirically. Values of "m" are given in Table II for a range of temperatures, and there is a general trend for "m" to decrease slightly with increasing temperature:

$$m = 0.7251 - 3.112 \times 10^{-4} \cdot (T) \qquad \text{Eq. [2]}$$
Where T = Temperature (°C)

This trend is illustrated in Figure 5. Equation [2] is not expected to be valid in the near-threshold regime where microstructural features and crack closure tend to dominate stress ratio effects.

It will be noted in Table II that negative stress ratios were employed at several test temperatures. Although it is difficult to visualize the mechanism by which negative loads closing a crack could contribute to crack growth, such is the case for some alloys, including Alloy 718. Negative stress ratios are entered into Equation [1] in the algebraic sense.

Crack Growth Under Static Loads

The objective of this paper is to review crack growth in Alloy 718 under cyclic loadings, and in general crack growth under static loadings is beyond the scope of this paper. Nevertheless, several studies have dealt with crack growth under static loads at elevated temperatures [26, 29, 36, 45-49] and since such loadings are input into some schemes to correlate cracking under complex conditions, they are briefly reviewed here. Cracks readily propogate in Alloy 718 under static loadings in air over the temperature range 425°C [29] to 760°C [46], and in general, time-based crack growth rates (da/dt) increase with increasing temperature. Reference 45 obtained a very linear Arrhenius plot of log(da/dt) versus reciprocal absolute temperature in air at 566°C, 593°, 649°, 677° and 704°C, and obtained an apparent activation energy of 47 kcal/mol. Reference 29 studying temperatures of 425°, 540°, and 650°C in air also obtained 47 kcal/mol. Reference 46 employed several unit loadings and observed that the crack growth curves shifted to the right as unit loadings increased (similar to the effect shown in Figure 4 for cyclic loadings). Reference 36 also noted that crack growth rates observed early in a test were of a transient non-steady state nature and could not be correlated using K. These observations again put into question the effectiveness of LEFM relationships in correlating crack growth behavior under static load and hold-time conditions at temperatures in excess of 538°C. However, use of other parameters (e.g., nominal stress, J, J*, and C*) have not necessarily improved the correlation [46, 49].

Crack Growth Under Complex Thermal-Mechanical Cycling

The majority of FCP experiments are conducted employing constant load amplitudes and isothermal conditions, yet many actual structural applications involve non-constant loadings and nonisothermal conditions. Several studies [38, 52-54] have employed complex loading sequences and/or non-isothermal conditions in attempts to develop correlation schemes. For example, Reference 50 studied sustained load crack growth while the temperature cycled between 537°C and 649°C. A linear cumulative damage model adequately (conservatively) predicted crack growth rates. References 52 and 54 cycled both loads and temperatures, and again a linear cumulative damage model which sums cycle-dependent and time-dependent terms adequately predicted crack growth. Reference 53 compared the predictive abilities of two different models for variations in frequency, stress ratio, and hold-time at 649°C, and Reference 51 studied the superposition of minor high-frequency high stress ratio cycles upon lower frequency major cycles. Most of the studies on complex thermal and/or mechanical cycling have also included models with which the behavior could be predicted.

MATERIAL VARIABLES

Heat-to-Heat Variations

Several studies have tested more than one heat of Alloy 718 and noted that, in some cases, there are heat-to-heat variations in the FCP behavior [8, 18, 28, 55, 56]. In the most extensive study, Reference 18 tested seven different heats from four different producers representing four different product forms, two different melting practices and two different heat-

treatments. Tests were conducted at 24°, 316°, 427°, 538° and 649°C. Heat-to-heat variations were noted, but the reason why a given heat would exhibit different FCP behavior was not obvious on the basis of chemical composition, mechanical properties, melting practice, product form, or microstructure. None of the other studies which noted heat-to-heat variations offered a consistent reason for the variations.

Effect of Product Form

Different product forms was one of the parameters considered in the previous section. One study [11] investigated potential product form variations by employing a single well-characterized heat in five different product forms: sheet, plate, bar, forging, and a weldment. By utilizing a single heat of material, compositional variations could also be eliminated. No difference was noted between the FCP behaviors of the four wrought product forms over the temperature range 24°-649°C, but FCP rates were generally higher in the weldment than in the wrought product forms.

Effect of Heat-Treatment

Alloy 718 derives its excellent strength properties as a result of precipitation heat-treatment. Several different heat-treatments have been developed for this alloy, and for this reason a large number of studies have studied the effect of heat-treatment upon the FCP behavior [2, 3, 6-8, 11, 16-18, 23, 28, 39, 55, 56]. Although there are several different heat-treatments, most studies have concentrated on three: the "conventional" heat-treatment (CHT), the "modified" heat-treatment (MHT), and the "Wilson" heat-treatment (WHT). These three treatments are given in Table III.

The FCP behavior of annealed Alloy 718 has been compared to that given the CHT at test temperatures of 24°, 316° and 538°C [2, 3, 18]. FCP rates in the annealed material were higher than in CHT material at all three temperatures.

The majority of studies have compared the FCP behavior of CHT material and MHT material [3, 7, 8, 11, 16-18, 28, 39, 56], and the various studies cover the temperature range 24° to 650°C. Almost without exception, FCP rates are higher in CHT material than in MHT material. Table III shows that the MHT employs a higher annealing temperature than the CHT, and this higher temperature is sufficient to put back into solution laves phase and δ phase precipitates, both of which have been shown to increase FCP rates [17, 18]. The higher annealing temperature of the MHT also results in some grain growth, and larger grains have been shown to produce lower FCP rates, particularly under hold-time conditions at elevated temperatures [22, 31].

A few studies have also compared the WHT to the CHT and/or the MHT. The WHT was originally developed to improve the notch rupture life, but it also produces lower FCP rates at elevated temperature than either the CHT or the MHT [23, 55, 56].

Reference 6 studied several combinations of solution treatment, cold-work, and aging time and temperature. Little difference was noted in the FCP behavior at room temperature, but more substantial differences were noted at -269°C and -196°C. Again, a higher solution annealing temperature dissolved grain boundary carbides and improved FCP behavior.

Although not a precipitation heat-treatment, Reference 3 studied long-term thermal aging in Alloy 718. Specimens given the CHT were then aged for 3000, 6000, and 12,000 hours at 538°C prior to FCP testing at 538°C. No effect of aging upon the FCP behavior was noted for any of the three times.

Effect of Microstructure

Dissolution of microstructural constituents such as Laves phase, δ-phase, and carbides during solution treatment, and the subsequent improvement in FCP behavior was discussed in the previous section. Another microstructural feature that can have a profound influence upon FCP under hold-time conditions, is grain size. Reference 22 studied grain size effects at 538°C employing a 10.8-minute hold-time, and References 31 and 59 employed a 5-minute hold-time at 650°C. Grain sizes ranged from ASTM 5 (large grain) to ASTM 11.5 (fine grain) in Reference 22, and ASTM 3-4 to ASTM 6-8 in References 31 and 58. In general, both studies noted that FCP rates increased as grain size got smaller. However, both Reference 22 and References 31 and 57 found that the lowest FCP rates were associated with a "necklace" microstructure: large grains surrounded by necklaces of very small grains. An example of grain size effects is shown in Figure 6, with the fine-grain specimens exhibiting higher rates, large-grain specimens lower rates, and the specimen with the necklace structure (Heat G forging) the lowest rates of all. Grain size effects have also been noted under continuous cycling (0.33 Hz) at 428°C, with larger grains again producing lower FCP rates [58].

The modified heat treatment (MHT), discussed earlier, produces a larger grain size than the conventional heat treatment (CHT) by virture of the higher solution annealing temperature. It has been suggested [22, 59] the lower FCP rates associated with the MHT during continuous cycling (no hold-times) may be a result of the larger grain size. Reference 59, noting that coarse grained material results in much rougher fracture surfaces at near threshold growth rates, suggests that roughness-induced crack closure may explain the observed effect of grain size.

Different microstructure-related modes of cracking are observed over a wide range of ΔK [8, 17, 18]. At low ΔK (below 20 MPa$\sqrt{m}$), fracture surfaces display a highly faceted or cleavage-like appearance indicative of crystallographic fracture along intense heterogeneous deformation bands. At intermediate levels of ΔK (20-60 MPa$\sqrt{m}$), well-defined striations are observed. The striation spacing is generally in good agreement with macroscopic FCP rates [8,18], and this is illustrated in Figure 7 for test temperatures of 24° and 538°C. Note also the reasonably good agreement between the observed striation spacing and the relationship proposed by Bates and Clark [60]. At higher levels of ΔK (greater than 60 MPa$\sqrt{m}$), fracture surfaces generally exhibit rather poorly defined microvoids coupled with large striations. At higher temperatures and lower cyclic frequencies (or longer hold-time) there is a transition from transgranular to intergranular crack propagation, with the transition level of ΔK decreasing with increasing temperature and hold-time.

Effect of Thickness

There is often a difference between the thickness of a given structural component and that of the test specimens employed to characterize the FCP behavior. A few studies have investigated potential thickness effects in Alloy 718. Reference 11 studied thicknesses between 1.57 and 12.7 mm over the temperature range 24°-538°C in air and found no effect of thickness. Similarily, Reference 61 observed the same trend for thicknesses between 6.3 and 25.4 mm in air at 650°C. Two studies [61, 62] also observed no thickness effects in air under static loads at 540° and 595°C, respectively. On the other hand, Reference 20 found thickness to be very critical under static loads in vacuo at 649°C.

Crack Growth Threshold

The FCP threshold, ΔK_{th}, is of considerable interest in applications where a large number of low amplitude cycles are anticipated, and for this reason several studies have had the objective of characterizing ΔK_{th} [15, 20, 25, 59, 63-65]. An example of near-threshold FCP behavior is shown in Figure 8. Note that the superiority of the MHT disappears in the near-threshold regime, and that the MHT material actually displays a slightly lower value of ΔK_{th} (generally taken to be the value of ΔK at $da/dN = 10^{-7}$ mm/cycle). However, generalization about the relative advantages of the CHT and MHT in the near-threshold regions should be avoided since Reference 59, employing a different heat of Alloy 718, observed the opposite trend at the same temperature. Clearly, microstructural features in addition to grain size must also be influencing near-threshold FCP behavior.

Similarily, apparent differences are observed regarding the role of environment upon ΔK_{th}. Reference 15, studying near-threshold behavior at 24° and 538°C, found ΔK_{th} to be lower in a helium environment than in air. This observation is consistent with the concept of oxide-induced crack closure producing higher closure loads (and hence a higher ΔK_{th}) in the air environment. On the other hand, Reference 20 found higher values of threshold K under static loads in vacuo at 649°C than in air at the same temperature. This observation was consistent with the much more extensive crack tip plasticity observed in vacuo, thereby suggesting that crack tip blunting led to a higher value of threshold.

ΔK_{th}, has also been observed to decrease with increasing R [15, 63-65], a trend observed in most metallic alloys. Again, this trend is compatible with crack closure arguements, although one study [58] argues that closure is not responsible for this trend. It is also observed [63-65] that, at elevated temperature, ΔK_{th} increases with increasing temperature. This trend is compatible with the notion of oxide-induced crack closure; the oxidation rate increases with temperaure hence producing thicker oxide layers. Reference 65 notes that the apparent activation energy for threshold crack arrest in comparable to the apparent activation energy for oxidation.

One practical difficulty that the above observations poses is the fact that ΔK_{th} in air or other aggressive environments may not be a unique material property. The evidence that ΔK_{th} is influenced by oxide-induced crack closure also suggests that ΔK_{th} may also then be a function of crack length and crack type (e.g., through-thickness crack as opposed to a surface crack). In fact, this author has observed that ΔK_{th} of alloy 718 is not a unique value in air at 427°C for large specimens where multiple crack arrest events can be achieved on the same specimen. Clearly, more study is necessary before ΔK_{th} can be considered a unique material property in aggressive environments.

Crack Growth in Alloy 718 Welds

Many Alloy 718 structural components are joined by welding, hence many studies have addressed the FCP behavior of Alloy 718 weldments [3, 7, 11, 16, 17, 26, 66-70]. A wide range of temperatures has been studied (-253°C to 649°C), and in general, FCP rates in the weldments are equivalent to those in base metal or are faster than those in base metal. FCP rates in weldments given the MHT are less than in those given the CHT, and this has been attributed to the dissolution of the laves phase due to the higher annealing temperature of the MHT [3, 7, 11, 16, 17]. The presence of welding defects (porosity, inclusions, and lack-of-fusion) did not influence the overall macroscopic FCP rates in Alloy 718 weldments at 24°C and 538°C [68].

It is occassionaly necessary to join Alloy 718 to other alloys through welding, and one study [66] addressed the FCP behavior of Alloy 718 welded to Alloy 600 or Type 316 stainless steel. In both cases, Alloy 82 filler metal was employed. FCP tests were conducted at 427°C and 538°C, and in general, crack growth rates in the weld metal and fusion zone were not significantly different from those in the Alloy 718 base metal.

ENVIRONMENTAL VARIABLES

Effect of Environment

Perhaps the single most important variable in influencing the FCP behavior of Alloy 718 is the environment, either liquid or gaseous. For this reason a large number of studies have been devoted to environmental effects. Besides air, the environments that have been studied include vacuum [9, 19, 20, 31, 39, 48, 57, 75], hydrogen [21, 71, 72, 74], helium [15, 23, 71, 74], nitrogen [9, 74], oxygen [9], argon [21], carbon dioxide [74], and liquid sodium [73]. In addition, Reference 40 characterized FCP behavior in shop cleaning solvent plus water contaminated with several salts, while Reference 74 studied FCP in air, helium hydrogen, each contaminated with other gasses (water vapor, O_2, CH_4, H_2S, SO_2). Although FCP tests were not conducted, Reference 76 studied the stress-corrosion-cracking behavior of Alloy 718 in a pressurized water reactor environment at 288°C.

As discussed earlier, FCP rates in vacuo are generally lower than in air under the same conditions, and the same observation appears to be true for helium and argon environments as well. FCP rates in nitrogen at 650°C appear to be only slightly higher than in vacuo, while those in oxygen at 650°C are intermediate between air vacuum rates. Some of the gaseous impurities studied by Reference 74 produced substantial increases in da/dN, although they did not produce significant corrosion on unstressed samples.

It is clear, when comparing FCP behavior in vacuo and in air, that air represents a relatively aggressive environment. It is generally considered that oxygen is the species responsible for the aggressive nature of air [19, 23, 31, 57]. It has been suggested that oxygen diffusion along grain boundaries promotes a reduction in grain boundary ductility [57], inhibition of planar slip [19], and an acceleration of cavity formation [23].

Reference 21, testing in hydrogen at a pressure of 34.5 kPa and cyclic frequency of 5 Hz found that FCP rates increased with temperature between -52°C and 303°C, and at room temperature noted that FCP rates in hydrogen and argon were approximately the same. On the other hand, Reference 71 testing at room temperature in hydrogen at a pressure of 34.5 MPa and a frequency of 1 Hz observed higher FCP rates in hydrogen than in helium, and suggested that the lack of FCP enhancement noted in Reference 21 was due to low H_2 pressure and the higher frequency. Reference 71 showed that, at room temperature, FCP rates in hydrogen increased with hydrogen pressure between 68.9 kPa and 68.9 MPa, and also increased with decreasing cyclic frequency over the range 0.1 Hz to 1 Hz. Reference 72 noted high crack growth rates in Alloy 718 tested under static loads in a hydrogen environment.

Effect of Neutron Irradiation

Although not part of the liquid or gaseous environment, neturon irradiation can be considered part of the total operational environment for components operating within a nuclear reactor. Several studies have addressed the effects of neutron irradiation upon the FCP behavior of Alloy 718 base metal [32, 33, 37, 69, 77] and weldments [69]. In general, irradiation has

little or no effect upon FCP behavior when the irradiation and test temperatures are both about 427°C [32, 69, 77], although weldments given the CHT exhibit higher FCP rates in the irradiated condition [69]. On the other hand, when the irradiaton and test temperatures are both about 650°C, neutron irradiation produces a significant increase in FCP rates [33, 37].

Neutron irradiation also tends to accelerate hold-time effects in Alloy 718 both at 427°C [32] as well as at 650°C [33, 37].

SUMMARY

This paper has reviewed the available literature on FCP in Alloy 718. Alloy 718 is a very complex alloy, and its response to a wide range of variables is itself quite complex. This alloy is very widely used in a variety of applications as evidenced by the large number of publications on FCP behavior. The large number of such publications necessitated that this review could not deal with them in detail, and this review is more of a "road map" showing the reader where greater detail can be obtained.

REFERENCES

1. C. M. Hudson, NASA TN D-2743, National Aeronautics and Space Administration, 1965.*
2. L. A. James, J. Engng. Matls. & Techol., Vol. 95, 1973, pp. 254-256.
3. L. A. James, HEDL-TME 75-80, Westinghouse Hanford Co., 1975.*
4. P. L. Tobler, Cryogenics, Vol. 16, 1976, pp. 669-674.
5. P. Shahinian and K. Sadananda, 1976 ASME-MPC Symposium on Creep-Fatigue Interaction, pp. 365-390, ASME, 1976.
6. W. A. Logsdon, R. Kossowsky and J. M. Wells, Advances by Cryogenic Engineering, Vol. 24, pp. 197-209, Plenum Pub. Co., New York, 1977.
7. L. A. James, Weld. J. Res. Suppl., Vol. 57, 1978, pp. 17s-23s.
8. W. J. Mills and L. A. James, ASME Paper 78-WA/PVP-3, 1978.
9. P. Shahinian and K. Sadananda, Engineering Aspects of Creep, Vol. 2, Paper C239/80, I. Mech. E, London, 1980.
10. L. A. James and W. J. Mills, Fatigue Crack Growth Measurement and Data Analysis, ASTM STP-738, pp. 70-82, 1981.
11. L. A. James, J. Engng. Matls. & Techol., Vol. 103, 1981, pp. 234-239.
12. M. Clavel and A. Pineau, Matls. Sci. & Engng., Vol. 55, 1982, pp. 157-171.
13. M. Clavel and A. Pineau, Matls. Sci. & Engng., Vol. 55, 1982, pp. 173-180.
14. M. Clavel and A. Pineau, Met. Trans., Vol. 9A, 1978, pp. 471-480.
15. J. L. Yuen, C. G. Schmidth and P. Roy, Fatigue & Fract. Engng. Matls. & Struct., Vol. 8, 1985, pp. 65-76.
16. L. A. James and W. J. Mills, J. Engng. Matls. & Technol., Vol. 107, 1985, pp. 34-40.

17. W. J. Mills and J. A. James, J. Engng. Matls. & Technol., Vol. 107, 1985, pp. 41-47.

18. L. A. James and W. J. Mills, Engng. Fract. Mech., Vol. 22, 1985, pp. 797-817.

19. H. H. Smith and D. J. Michel, Met. Trans., Vol. 17A, 1986, pp. 370-374.

20. M. Stucke, M. Khobaib, B. Majumdar, and T. Nicholas, Advances in Fracture Research, pp. 3967-3975, Pergamon Press, 1984.

21. R. P. Wei, K. Klier, G. W. Simmons, R. P. Gangloff, E. Chornet, and R. Kellerman, NASA-CR-140008, National Aeronatucis and Space Administration, 1974.*

22. L. A. James, Engng. Fract. Mech., Vol. 25, 1986, pp. 305-314.

23. S. Floreen and R. H. Kane, Fatigue & Fract. Engng. Matls. & Struct., Vol. 2, 1980, pp. 401-412.

24. T. Weerasooriya, AFWAL-TR-87-4038, Air Force Wright Aeronautical Laboratories, 1987.*

25. N. E. Ashbaugh and T. Nicholas, 20th National Fracture Mechanics, ASTM STP 1020, in press 1989.

26. H. G. Popp and A. Coles, AFFDL TR 70-144, pp. 71-86, Air Force Flight Dynamics Laboratory, 1970.*

27. A. Coles, R. E. Johnson, and H. G. Popp, J. Engng. Matls. & Technol., Vol. 98, 1976, pp. 305-315.

28. H. H. Smith and D. J. Michel, Ductility and Toughness Considerations in Elevated Temperature Service, Series MPC-8, pp. 225-246, ASME 1978.

29. K. Sadananda and P. Shahinian, J. Engng. Matls. & Technol., Vol. 100, 1978, pp. 381-387.

30. V. Shahani and H. G. Popp, NASA-CR-159433, National Aeronautics and Space Administration, June 1978.*

31. J. P. Pedron and A. Pineau, Memoires et Etudes Scientifiques Revue de Metallurgie, Vol. 85, 1983, pp. 665-674.

32. D. J. Michel and H. H. Smith, J. Nucl. Matls., Vol. 122-123, 1984, pp. 153-158.

33. H. H. Smith and D. J. Michel, J. Nucl. Matls., Vol. 137, 1985, pp. 81-85.

34. T. Nicholas, T. Weerasooriya, and N. E. Ashbaugh, Fracture Mechanics: Sixteenth Symposium, ASTM STP 868, pp. 167-180, 1985.

35. T. Nicholas and T. Weerasooriya, Fracture Mechanics: Seventeenth Volume, ASTM STP 905, pp. 155-168, 1986.

36. A. Diboine and A. Pineau, Fatigue & Fract. Engng. Matls. & Struct., Vol. 10, 1987, pp. 141-151.

37. H. H. Smith and D. J. Michel, J. Nucl. Matls., Vol. 149, 1987, pp. 109-112.

38. T. Weerasooriya and T. Nicholas, Fracture Mechanics: Eighteenth Symposium, ASTM STP 945, pp. 181-191, 1988.

39. K. Sadananda and P. Shahinian, Creep-Fatigue-Environment Interactions, Met. Soc. of AIME, pp. 86-111, 1979.

40. R. R. Ferguson and R. C. Berryman, AFML-TR-76-137, Air Force Materials Laboratory, 1976.*

41. P. Shahinian and K. Sadananda, J. Engng. Matls. & Technol., Vol. 101, No. 2, pp. 224-230, 1979.

42. K. Sadananda and P. Shahinian, Fracture Mechanics; Twelfth Conference, ASTM STP 700, pp. 152-163, 1980.

43. T. Nicholas and N. E. Ashbaugh, Fracture Mechanics: Nineteenth Symposium, ASTM STP 969, pp. 800-817, 1987.

44. E. K. Walker, AFFDL TR 70-144, pp. 225-233, Air Force Flight Dynamics Laboratory, 1970.*

45. S. Floreen, Met. Trans., Vol. 6A, 1975, pp. 1741-1749.

46. K. Sadananda and P. Shahinian, Met. Trans., Vol. 8A, 1977, pp. 439-449.

47. K. Sadananda, Met. Trans., Vol. 9A, 1978, pp. 635-641.

48. K. Sadananda and P. Shahinian, Matls. Sci. & Engng., Vol. 43, 1980, pp. 159-168.

49. K. Sadananda and P. Shahinian, Micro and Macro Mechanics of Crack Growth, Met. Soc. of AIME, pp. 119-130, 1981.

50. G. K. Haritos, D. L. Miller, and T. Nicholas, J. Engng. Matls. & Technol., Vol. 107, 1985, pp. 172-179.

51. S. Venkataraman, T. Nicholas, and N. E. Ashbaugh, Fractography of Modern Engineering Materials: Composites and Metals, ASTM STP 948 pp. 383-399, 1987.

52. M. L. Heil, T. Nicholas, and G. K. Haritos, Thermal Stress, Material Deformation, and Thermo-Mechanical Fatigue, PVP Vol. 123, pp. 23-29, ASME, 1987.

53. G. K. Haritos, T. Nicholas, and G. O. Painter, Fracture Mechanics: Eighteenth Symposium, ASTM STP 945, pp. 206-220, 1988.

54. T. Nicholas, M. L. Heil, and G. K. Haritos, Int. J. Fracture, (in press).

55. K. Sadananda and P. Shahinian, NRL Memorandum Report 3727, Naval Research Laboratory, 1978.*

56. K. Sadananda and P. Shahinian, Res Mechania, Vol. 1, 1980, pp. 109-128.

57. J. P. Pedron and A. Pineau, Matls. Sci. & Engng., Vol. 56, 1982, pp. 143-156.

58. R. H. Van Stone, Matls. Sci. & Engng., Vol. A103, 1988, pp. 49-61.

59. J. L. Yuen and P. Roy, Scripta Met., Vol. 17, 1985, pp. 17-22.

60. R. C. Bates and W. G. Clark, ASM Trans. Quarterly, Vol. 62, 1969, pp. 380-389.

61. K. Sadananda and P. Shahinian, Characterization of Materials for Service at Elevated Temperatures, Series MPC-7, pp. 107-127, ASME, 1978.

62. S. Floreen, Engng. Fract. Mech., Vol. 11, 1979, pp. 55-60.

63. J. L. Yuen, PhD Dissertation, Dept. of Matls. Sci. & Engng., Stanford University, June 1982.

64. J. L. Yuen and P. Roy, Fatigue Crack Growth Threshold Concepts, Met. Soc. of AIME, pp. 185-203, 1983.

65. J. L. Yuen, P. Roy and W. D. Nix, Met. Trans., Vol. 15A, 1984, pp. 1769-1775.

66. D. E. Pettit, C. E. Feddersen and H. Mindlin, NASA CR-101942, National Aeronautics and Space Administration, 1969.*

67. L. A. James, HEDL-TME 76-93, Westinghouse Hanford Co., March 1977.*

68. L. A. James and W. J. Mills, Int. J. Press. Vessels & Piping, Vol. 9, 1981 pp. 367-383.

69. L. A. James, J. Nucl. Matls., Vol. 136, 1985, pp. 91-96.

70. R. G. Forman, NASA TN D-7665, National Aeronautics and Space Administration, 1974.*

71. R. J. Walter and W. T. Chandler, NASA-CR-124410, National Aeronautics and Space Administration, 1973.*

72. R. G. Forman, NASA TN D-7952, National Aeronautics and Space Administration, 1975.*

73. W. J. Mills and L. A. James, J. Engng. Matls. & Technol., Vol. 101, 1979, pp. 205-213.

74. S. Floreen and R. H. Kane, Met. Trans., Vol. 10A, 1979, pp. 1745-1751.

75. K. Sadananda and P. Shahinian, Metals Technol., Vol. 9, 1982, pp. 18-25.

76. M. T. Miglin and H. A. Domain, J. Matls. Engng., Vol. 9, 1987, pp. 113-132.

77. D. J. Michel and H. H. Smith, J. Nucl. Matls., Vol. 85-86, 1979, pp. 845-849.

* Report available from the U.S. Department of Commerce, National Technical Information Service, Springfield, VA 22161.

TABLE I

RANGE OF TEMPERATURES STUDIED

Reference No.	Temperature Range
1	-78°, 27°, 288°C
2	24°, 316°, 538°C
3	24°, 316°, 427, 538°, 649°C
4	-269°, -197°, -78°, 22°C
5	538°, 649°, 760°C
6	-269°, -197°, 24°C
7	24°, 427°, 538°, 649°C
8	24°, 316°, 427°, 538°, 649°C
9	24°, 538°, 650°C
10	24°, 538°C
11	24°, 316°, 427°, 538°, 649°C
12,13	25°, 550°, 650°C
14	25°, 550°C
15	24°, 538°C
16,17	24°, 316°, 427°, 538°, 649°C
18	24°, 316°, 427°, 538°, 649°C
19	593°, 649°C

TABLE II

Range of Stress Ratios Studied

Temperature	Range of R	Walker Exponent "m"	Reference
-78°C	$-0.2 < R < 0.78$	0.70*	1
24	$0.08 < R < 0.5$	0.75*	40
27	$-0.2 < R < 0.78$	0.75*	1
204	$0.08 < R < 0.5$	0.60*	40
288	$-0.2 < R < 0.78$	0.75*	1
427	$0.05 < R < 0.5$	0.50	3
504	$-1 < R < 0.818$	0.55	27
538	$0.05 < R < 0.667$	0.60	3
649	$0.1 < R < 0.9$		25, 43
650	$0.2 < R < 0.8$		39, 42
650	$0.05 < R < 0.8$		41

*In many cases, Walker Equation exponents were not reported by the individual authors: they were determined herein using the data presented.

TABLE III

Summary of Common Heat-Treatments

CONVENTIONAL HEAT-TREATMENT (CHT)
Anneal at 954°C, air cool to room temperature.
Age 8 hours at 718°C, furnace cool to 621°C and hold at 621°C for a total aging time of 18 hours.

MODIFIED HEAT-TREATMENT (MHT)
Solution anneal 1 hour at 1093°C, cool to 718°C at 55°C/hour.
Age 4 hours at 718°C, cool to 621°C at 55°C/hour.
Age 16 hours at 621°C, air cool to room temperature.

WILSON HEAT-TREATMENT (WHT)
Anneal 10 hours at 926°C, furnace cool.
Age 48 hours at 734°C.

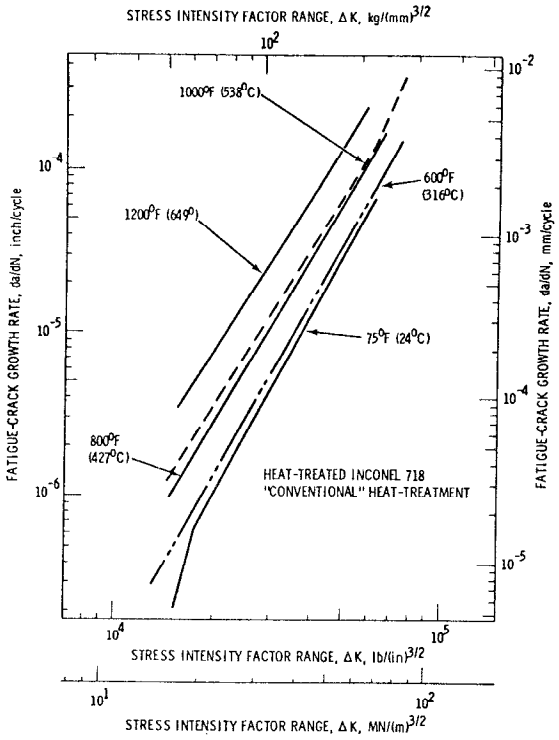

Figure 1: Effect of Temperature Upon the Fatigue Crack Propagation Behavior in Air (From Reference 3)

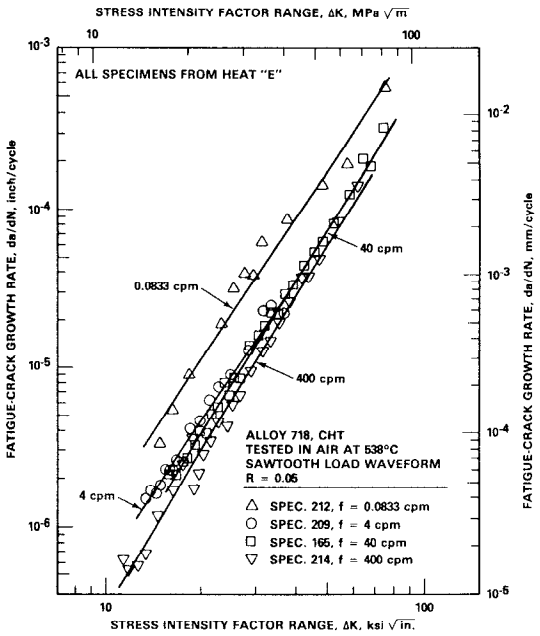

Figure 2: Effect of Cyclic Frequency Upon the Fatigue Crack Propagation Behavior in Air at 538°C. (From Reference 22)

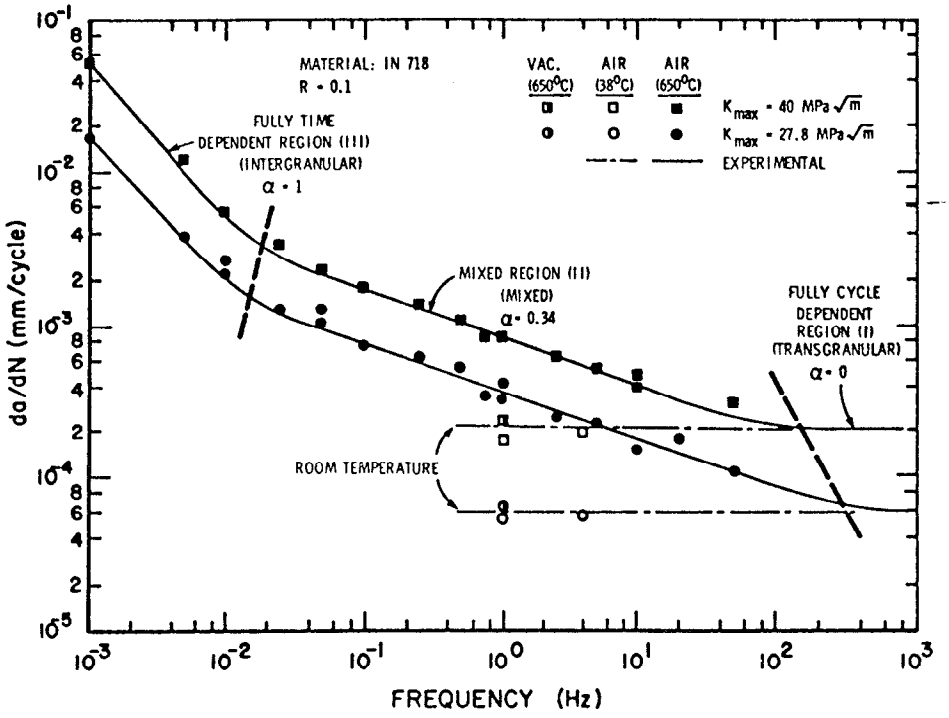

Figure 3: Cyclic Frequency Effects in an Air Environment at 650°C at ΔK = 40 MPa√m. (from Reference 24)

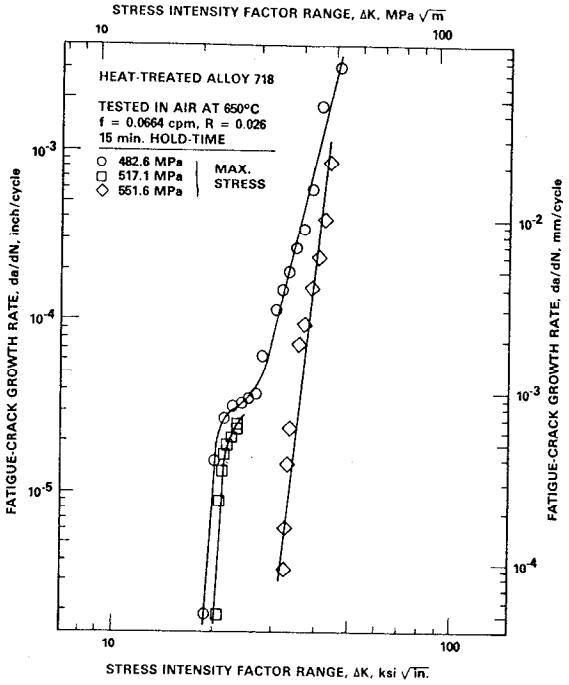

Figure 4: Effect of Stress Level Upon Fatigue Crack Propagation Behavior Under Hold-Time Conditions in air at 650°C. (From Reference 30)

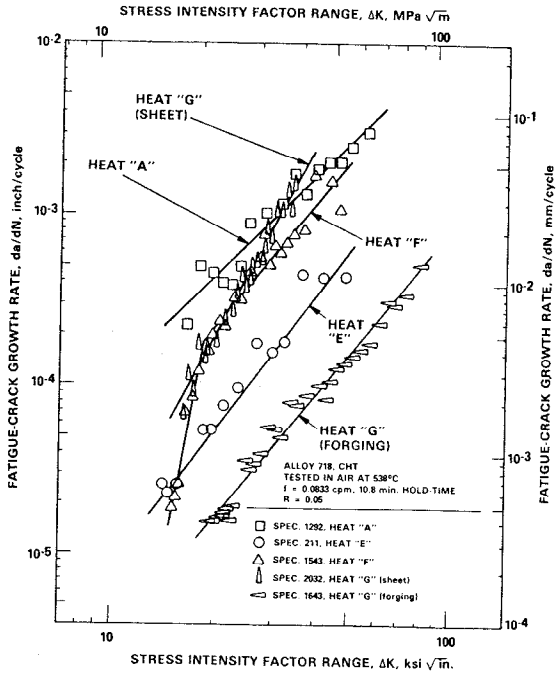

Figure 6: Effect of Grain Size Upon the Fatigue Crack Propagation Behavior at 538°C Under Hold-Time Conditions. ASTM grain sizes: Heat A = 11.5, Heat E = 5, Heat F = 10.5, Heat G sheet = 10, Heat G Forging = 5 with a "necklace". (from Reference 22).

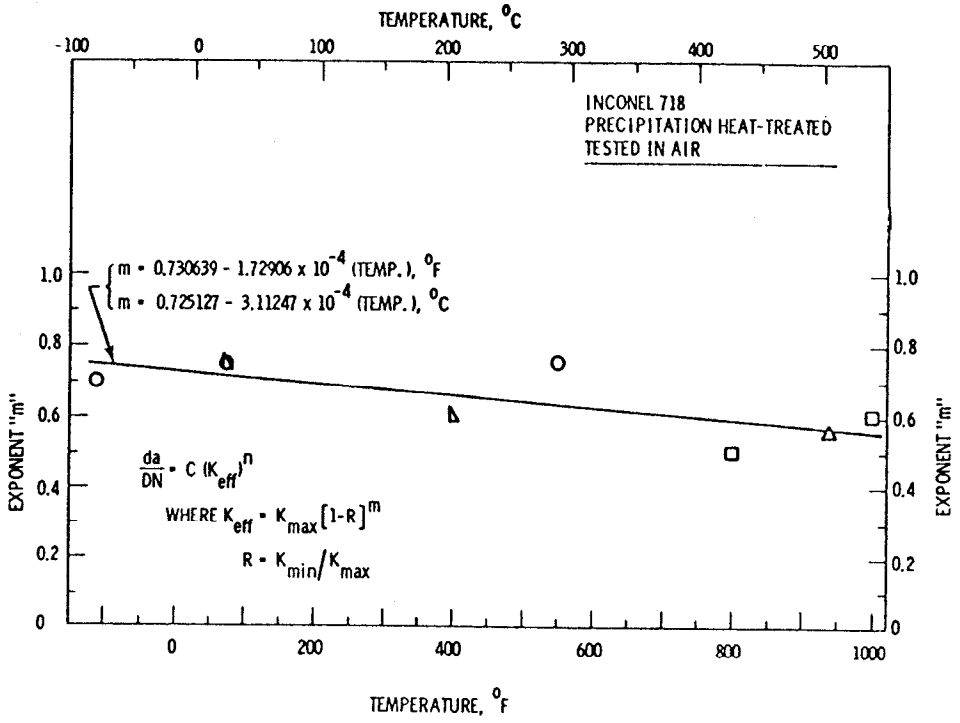

Figure 5: Effect of Temperature Upon the Exponent in the Stress Ratio Correlation of Equation [1].

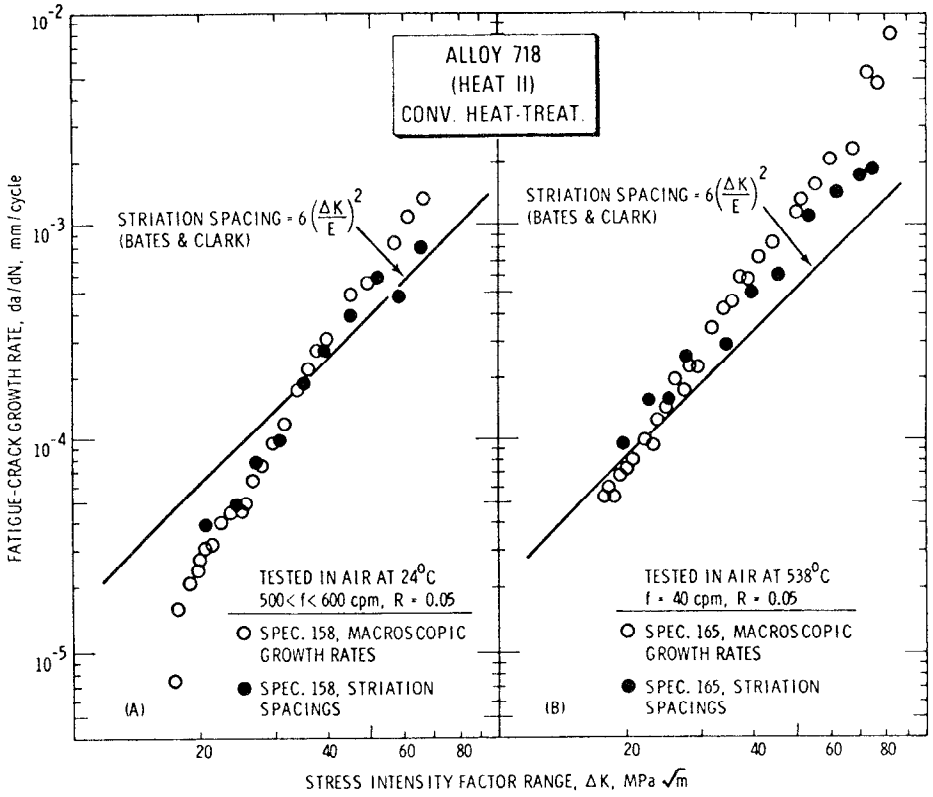

Figure 7: Correlation Between Microscopic Striation Spacings and Macroscopic Fatigue Crack Growth Rates at 24° and 538°C. (from Reference 8).

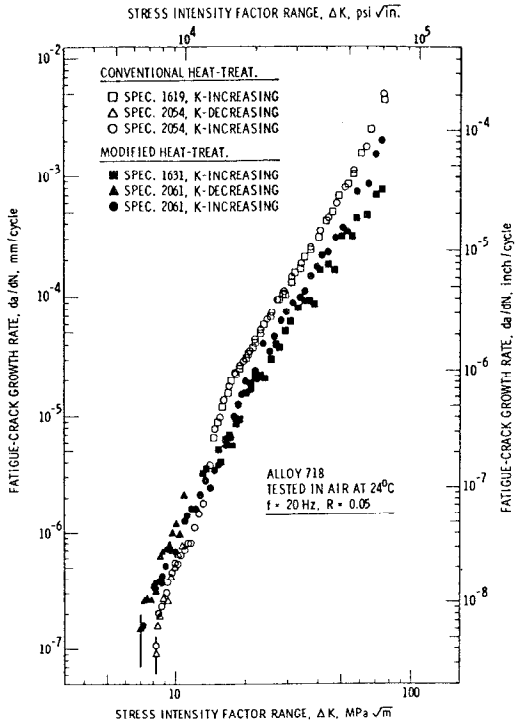

Figure 8: Near-Threshold Fatigue Crack Propagation Behavior For Two Different Heat Treatments at Room Temperature. (Data produced by the author while at Westinghouse Hanford Co.)